Electrochemical scanning tunneling microscopy study of the electrochemical behavior of naked and *n*-alkanethiol-modified Au(111) surfaces in F^-- and CN^--containing electrolyte solutions

Yin-Quan Li, Orawon Chailapakul, and Richard M. Crooks[a)]
Department of Chemistry, Texas A&M University, College Station, Texas 77843-3255

(Received 7 October 1994; accepted 19 December 1994)

We report an electrochemical scanning tunneling microscopy (ECSTM) study of CN^-- and F^--induced etching of naked and *n*-alkanethiol-modified Au(111) surfaces. We use electrochemical methods to activate or deactivate etching of the Au surface, and we monitor changes in surface topography simultaneously using STM. In F^--containing electrolytes we have observed that the STM tip can induce surface–atom diffusion in the electrochemical environment thereby enhancing surface pitting, island growth, and step edge movement. At potentials more negative than −150 mV (vs Ag/AgCl) the tip selectively removes Au atoms from surface defects and enhances growth on terraces. Similarly, we have found that the STM tip can profoundly alter the CN^--induced dissolution rate of Au. On naked Au surfaces held at extreme negative potentials, no CN^- etching of the surface occurs. However, at slightly more positive potentials the surface is homogeneously etched. At intermediate potentials the area under the scanning STM tip is selectively etched at positive tip biases, but at slightly more negative biases etching proceeds less rapidly in the scanned region. Finally, when the Au(111) surface is modified with a single self-assembled monolayer (SAM) of organomercaptan molecules, surface etching processes are dramatically attenuated regardless of the substrate potential or tip bias.

I. INTRODUCTION

There have been a number of electrochemical scanning tunneling microscopy (ECSTM) studies of metal dissolution in electrolyte solutions.[1–4] Our principal goal here, however, is to report on the opposite process: etching inhibition. A common practice for preventing corrosion of metals is to coat the surface with a relatively thick film such as paint, a polymer, or a metal oxide. However, for applications in which the lateral dimensions of patterned features are in the nanometer regime, it may not be practical to use micron-thick films. In contrast, ultrathin organic films such as self-assembled monolayers (SAMs), which spontaneously form 10–30-Å-thick films on Au substrates, provide high-quality barriers to substrate corrosion reactions.[5–9] We[10–13] and others[14–21] have previously studied organomercaptan SAMs confined to Au surfaces using STM.

One of our principal interests is using the STM tip as a lithographic tool for creating patterns in SAMs, which we have found to be excellent resist materials.[12,13,22] For example, we have shown that STM-tip-etched patterns can be selectively metalated with Cu using a low-temperature chemical-vapor deposition (CVD) method.[13] This, and other studies of SAM-passivated surfaces,[11,22–25] have suggested that SAMs nearly completely passivate metal surfaces: even molecular-scale defects are absent over micron-scale areas.[24,25]

Previous STM analyses of SAMs were performed either in air or vacuum, and although these studies permit direct visualization of the defect density and structure, it is more informative to study changes in surface topography as a function of the electrochemical surface potential in real time.[11,17,20–22] For example, here we find that a naked Au surface is topographically stable in up to 20 mM CN^- solutions at potentials negative of −770 mV vs Ag/AgCl. However, at open circuit or at potentials positive of −520 mV, Au dissolves in solutions containing concentrations of CN^- as low as 1 mM. Moreover, at potentials just positive of the onset of etching we find that when the STM tip is biased positive of the substrate etching is enhanced; however, negative tip biases reduce the etching rate. When the Au surface is modified with a well-ordered, compact *n*-alkanethiol SAM, we do not observe etching at any potential in either the scanned or unscanned areas.

II. EXPERIMENT

$HS(CH_2)_{15}CH_3$ (Aldrich, 92%) was purified by double distillation under reduced pressure. Other chemicals were of reagent grade quality or better and were used without further purification. Deionized water (Millipore Milli-Q purification system, >18 MΩ cm) was used throughout the experiments. All the electrolyte solutions used in the experiments were aqueous. Substrates were single crystal Au(111) facets obtained by melting the ends of 0.5-mm-diam Au wires (99.999%) in a H_2/O_2 flame.[10,26] The *n*-alkanethiol SAMs were prepared by immersing the freshly prepared substrates in 1 mM ethanolic solutions of $HS(CH_2)_{15}CH_3$ for the lengths of time indicated in the text. After immersion, the samples were rinsed thoroughly with ethanol and dried in a N_2 gas stream.

Microscopy was performed using a NanoScope III electrochemical scanning tunneling microscope (Digital Instruments, Santa Barbara, CA) equipped with an integral potentiostat. The custom-built electrochemical cell has a volume of 100 μl, and was designed to accommodate the Au ball

a)Author to whom correspondence should be addressed.

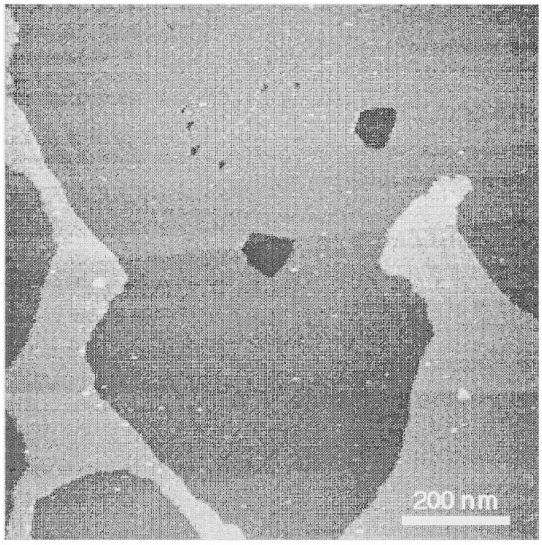

FIG. 1. 1 μm $\times$ 1 μm STM image of a Au(111) facet on a flame-annealed Au ball, acquired in 0.1 M KF at E_e=200 mV. V_b=100 mV; i_t=200 pA.

and enhance mechanical stability of the substrate to the maximum extent possible.[26] Pt wires, which were carefully cleaned with concentrated HNO_3, were used as both counter and quasi-reference electrodes (QRE). However, we calibrated the Pt-wire potential with respect to a Ag/AgCl reference electrode and converted the numerical value of the potential to this more standard reference using the common reference redox couple $Ru(NH_3)_6^{3+/2+}$. In 0.1 M KOH solutions we found $E_{Ag/AgCl}=E_{Pt}$ + 80 mV while in 0.1 M KF solution $E_{Ag/AgCl}=E_{Pt}$ + 300 mV. Our experience indicates that the potential of the Pt QRE is stable to within $\pm$20 mV for the duration of a 4 h ECSTM experiment. All electrolyte solutions were in equilibrium with air, and therefore contained about 1 mM O_2.[2]

The STM tips were either W wires etched in 1 M KOH or Pt/Ir wires (80:20) etched in 10 M NaOH. The Pt/Ir tips were insulated using either clear nail polish (Wet'n'Wild) or molten Apiezon wax to limit the Faradaic leakage current to less than 10 pA at 100 mV.[3,27] The W tips were always insulated using nail polish. The STM images were acquired in the constant-current mode; other relevant imaging conditions are given in the figure captions. A negative value of the tip bias indicates that the tip potential is negative of the substrate potential. All images are unfiltered, except for flattening and plane fitting to correct systematic errors introduced by the tube scanner and misorientation of the substrate, respectively.

III. RESULTS AND DISCUSSIONS

We typically observe atomically flat terraces $\sim$1 μm wide on flame-annealed Au balls (Fig. 1). The surface is composed primarily of a single atomic terrace with a few scattered one-atom-deep pits and a secondary terrace raised up by one atomic step (2.4 Å). The surface also contains two fairly large triangular pits, which confirms that it is of the (111) orientation.

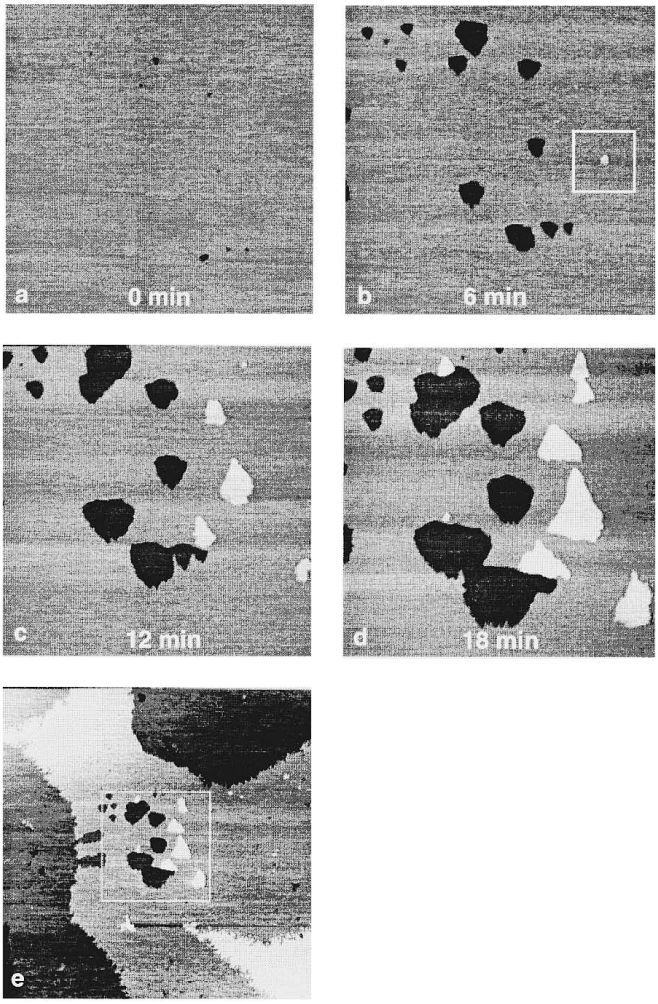

FIG. 2. Time-sequence STM images of Au(111) acquired in 0.1 M KF at E_e=$-$150 mV. V_b=100 mV; i_t=2 nA. (a)–(d) 1 μm $\times$ 1 μm. (e) 3 μm $\times$ 3 μm. The box in (b) indicates a raised feature. The box in (e) indicates the region scanned in (a)–(d).

A. Tip–substrate interactions in F^--containing solutions

The open circuit potential (OCP) of Au(111) in 0.1 M KF is about 200 mV vs Ag/AgCl. At potentials near the OCP surface features, which include pits, edges, and other defects, are fully stable under our typical imaging conditions (tip bias, $V_b\sim$100 mV, tunneling current, $i_t\sim$0.5 nA). However, when the electrode potential (E_e) is moved somewhat negative of the OCP, surface atoms in the vicinity of the scanning tip become mobile.

Figures 2(a)–2(d) show time-sequence STM images of a 1 μm$\times$1 μm region on a typical Au(111) surface in 0.1 M KF. The initial surface was a single flat terrace with a few small-diameter, one-Au-atom-deep pits less than 30 nm in diameter. After scanning this region of the surface for about 30 min at the OCP, we observed no substantial change in surface topography. We then moved the electrode potential to $-$150 mV immediately prior to obtaining the image shown in Figure 2(a). The data shown in Figure 2(b) were obtained after 6 min of continuous scanning at the same electrode potential. Although the depth of the pits do not change, they

increase in number and size, and we detect the presence of a single, small, raised island [The boxed feature in Figure 2(b)]. Interestingly, all the pits are more-or-less triangular in shape, and they have the same orientation, which is the result of a lowering of the surface symmetry from six-fold to three-fold by the second and third atomic layers of Au. We have previously discussed this phenomenon in detail.[11] It is interesting that the Au loss due to pit formation is not balanced by island growth; that is, there is an apparent net loss of Au from the surface. This suggests that the mechanism for Au atom mass transport must not be simple adatom diffusion as has been observed previously.[2] It seems reasonable to speculate that the missing atoms must either be at or near the perimeter of the scanned region, dissolved in the electrolyte solution, or transferred to the tip. We will show that the first of these possibilities is not correct. Since there is no evidence for Au dissolution at more positive potentials, we discount the second possibility. Thus, it seems that Au is transferred to the tip, although we have no direct evidence for such a phenomenon.

We obtained the image shown in Figure 2(c) 12 min after initiation of the experiment. Clearly, the pits are substantially larger and some have coalesced; however, their depth has remained constant. Moreover, more islands have formed on the main Au(111) terrace and the island previously present has grown substantially. Interestingly, the islands possess a somewhat triangular shape, and they are rotated 60° relative to the pits. An additional 6 min of scanning results in growth of both the pits and the islands [Fig. 2(d)]. We also observe that the island structures appear correlated to a particular pit, and they are always to the right of the pits. At the present time we cannot account for either of these observations.

A 3 μm $\times$ 3 μm scan taken after the image shown in Figure 2(d) reveals that the surface changes are restricted to the scanned area [Fig. 2(e)], and as a result we infer that the change in surface topography is driven by tip–substrate interactions. Although the pattern of the topographical changes differs from run to run, we observe the same general type of potential dependent surface mobility in other experiments at substrate potentials negative of -150 mV.

A complete disclosure of the mechanism responsible for the observed behavior awaits a better theoretical model of the overlapping electrochemical double layers of the tip and substrate. However, we note that in air and in vacuum the electric field between the tip and the substrate surface has previously been reported to induce surface reconstructions and atom diffusion.[28–32] The new observations we report indicate that this same phenomenon is operative in the electrochemical environment, which undoubtedly supports a totally different type of electric field between the tip and substrate than is present in air or vacuum. Moreover, in the electrochemical environment, the surface atom mobility also depends on the substrate potential. We believe that a very complex chemical structure in the tip–substrate gap results in this odd behavior, but we possess neither the experimental nor theoretical tools necessary to achieve a better understanding at the present time.

B. CN^- etching of naked Au(111)

In the previous section we demonstrated that Au(111) surfaces can be modified by the STM tip in F^--containing solutions. Now we turn our attention to a well-known chemical process: Au dissolution in alkaline CN^- solutions. Early electrochemical studies[33–36] have revealed the mechanism of the electrochemical dissolution of Au in alkaline CN^- solutions [Eqs. (1)–(3)].

$$\mathrm{Au}+\mathrm{CN}^- \rightarrow \mathrm{AuCN}^-_{\mathrm{ads}}, \tag{1}$$

$$\mathrm{AuCN}^-_{\mathrm{ads}} \rightarrow \mathrm{AuCN}_{\mathrm{ads}}+e^-, \tag{2}$$

$$\mathrm{AuCN}_{\mathrm{ads}}+\mathrm{CN}^- \rightarrow \mathrm{Au(CN)}^-_2 . \tag{3}$$

McCarley and Bard used STM to study the spontaneous dissolution of Au in a CN^- solution at open circuit.[2] In contrast, we set out to study CN^- etching on Au(111) surfaces under potential control. We start the experiment with a freshly annealed Au(111) surface immersed in an aqueous solution containing only 0.1 M KOH. We next move the electrode potential from the OCP, which is normally about -40 mV in 0.1 M KOH, to -770 mV through a series of small potential steps. We then add 1 mM CN^- to the cell with the electrode potential held at -770 mV, and then we scan the surface for 5 min. This treatment does not result in any significant changes to the substrate topography. This STM result is consistent with our data from companion electrochemical cyclic voltammetric experiments, which show that etching of the Au(111) surface does not occur in 1 mM CN^- when the potential is held negative of -600 mV.

When the electrode potential is moved to -520 mV, however, we observe rapid surface dissolution in the scanned region. When the potential is moved back to -770 mV, the etching stops and the new surface features again remain stable. Figure 3(a) shows an STM image of a 400 nm $\times$400 nm region on a naked Au(111) surface after it was etched for 3 min. The surface is rougher than a freshly annealed Au surface (compare with Figure 1). We then scanned this region for 7 min at $E_e=-820$ mV, and observed no significant topographical changes. However, when we moved the substrate potential from -820 to -520 mV, we immediately observed dramatic changes in the surface structure. An STM image of the area shown in Figure 3(a) taken 3 min after the potential step is shown in Figure 3(b). During the entire 3 min the STM tip was scanning the surface. A characteristic feature of the etching process under the influence of the tip is that the surface is now dominated by terraces of nearly uniform width that have their long dimension parallel to the fast scan direction of the STM tip. More interestingly, the step orientation changes from frame to frame: regardless of whether the tip scans from top to bottom or bottom to top the tip appears to move from upper steps to lower steps. This behavior is characteristic of layer-by-layer removal of Au terraces from the substrate at a frequency somewhat higher than the frame-capture speed. That the apparent steps are always nearly parallel to the fast scan direction clearly argues for a tip-assisted dissolution process.

To further compare the CN^- etching rate for scanned and unscanned areas, we recorded a 500 nm $\times$ 500 nm image of

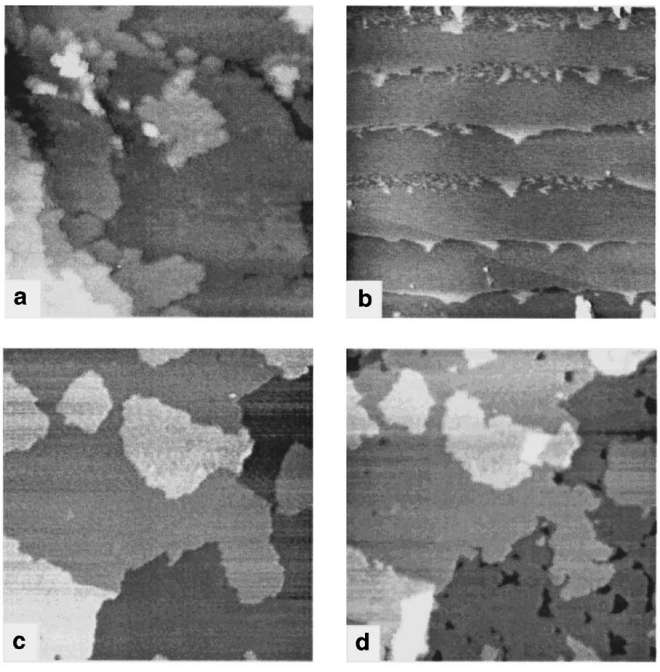

FIG. 3. 500 nm × 500 nm scans of Au(111) surfaces obtained in electrolyte solutions containing (a), (b): 0.1 M KOH + 2 mM KCN and (c), (d): 0.1 M KOH + 1 mM KCN. (a) $E_e = -820$ mV. (b) Same area as in (a) obtained 3 min after E_e was changed to −520 mV. The STM tip was continuously scanning this region throughout the 3 min duration of the etching experiment. (c) $E_e = -770$ mV. (d) Same area as in (c) obtained after the surface was etched at $E_e = -520$ mV for 3 min without being scanned. Scanning conditions: $i_t = 500$ pA for all the images. (a), (b) $V_b = 100$ mV. (c), (d) $V_b = 850$ mV.

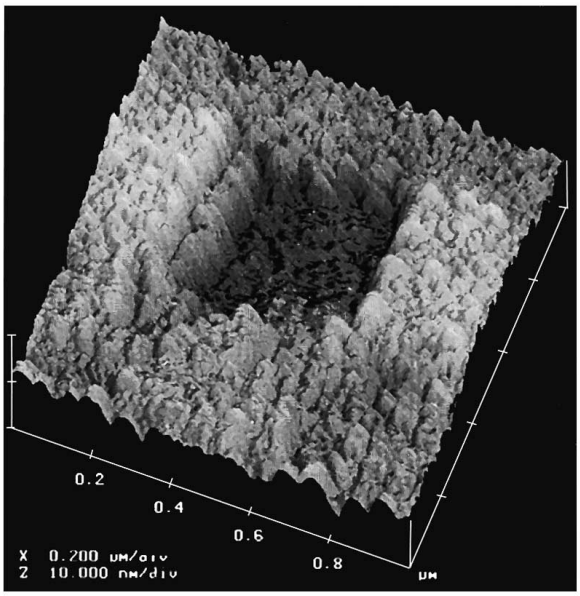

FIG. 4. Three-dimensional view of 1 μm × 1 μm scan of Au(111) obtained at $E_e = -770$ mV in 0.1 M KOH + 1 mM KCN. The central 400 nm × 400 nm area was scanned during etching at $E_e = -520$ mV. $V_b = 100$ mV; $i_t = 8$ nA.

Au(111) in 1 mM CN^- at $E_e = -770$ mV [Figure 3(c)]. Instead of scanning this region while etching, we effectively stopped the tip motion by reducing the scan rate to 0.1 Hz. Next, we stepped the electrode potential to −520 mV for 3 min, and then obtained the image shown in Figure 3(d) after changing the potential back to −770 mV. The larger scale features of the surface remain intact after this treatment, but the step-edge surface area increases and a number of triangular pits form on the terraces. The important point is, however, that a comparison of Figures 3(c) and 3(d) with Figures 3(a) and 3(b) clearly indicates that etching is enhanced by the presence ot the STM tip.

The dramatic effect of tip-enhanced etching is confirmed by Figure 4, which shows a large-scale image obtained after CN^- etching in the presence of tip scanning. We etched the Au surface at $E_e = -520$ mV in 1 mM CN^- for 2 min while scanning the central 400 nm × 400 nm region. The central region is preferentially etched, although the surrounding area also dissolves to a significant extent. When the electrode potential is moved back to −770 mV, the etching stops immediately, even in the surface region under the scanning tip. We have repeated this experiment many times on different samples; the results are fully reproducible. In accordance with the Nernst equation, the potential at which etching commences depends on the CN^- concentration. For 1 mM CN^- we observe fast etching at $E_e = -520$ mV. Etching slows considerably when the potential is moved to −670 mV. For 20 mM CN^- electrolyte solutions, we observe some etching at $E_e = -720$ mV, but there is no evidence for Au dissolution at $E_e = -770$ mV.

C. Tip bias dependence

The polarity of the tip-bias voltage also affects scan-induced Au dissolution in CN^--containing solutions; this effect is shown in Figures 5 and 6. We obtained images in Figure 5 using a −50 mV tip bias voltage (tip potential negative with respect to the substrate) in a 20 mM CN^--containing electrolyte solution. The images were obtained sequentially at intervals of about 1 min, which is the time required to capture a single frame. We recorded Figures 5(a)–5(e) with the electrode potential poised at −720 mV and then recorded Figure 5(f) at $E_e = -770$ mV. Figures 5(a)–5(e) indicate that there are no significant topographical changes in the surface features during scanning, but when we zoom out to display a larger area [Figure 5(f)], we find that the areas surrounding the scanned area show clear signs of etching: roughened terraces and significant pitting.

We next refocused the scan on the boxed area of Figure 5(f) and returned the electrode potential to −720 mV and changed the tip bias to +50 mV. We acquired the images shown in Figure 6 on the same time scale used to obtain the data shown in Figure 5. These figures indicate rapid dissolution of the surface under the influence of the positively biased tip. We cannot at present quantitatively account for the observed effects of enhanced etching at positive tip bias and reduced etching at negative bias, but it seems reasonable to speculate that the solution potential near the scanned region changes in the direction of the tip potential. That is, at positive tip bias, the local potential felt by the substrate is more positive than it would be in the absence of the tip. A similar effect has previously been observed during metal deposition.[3,37]

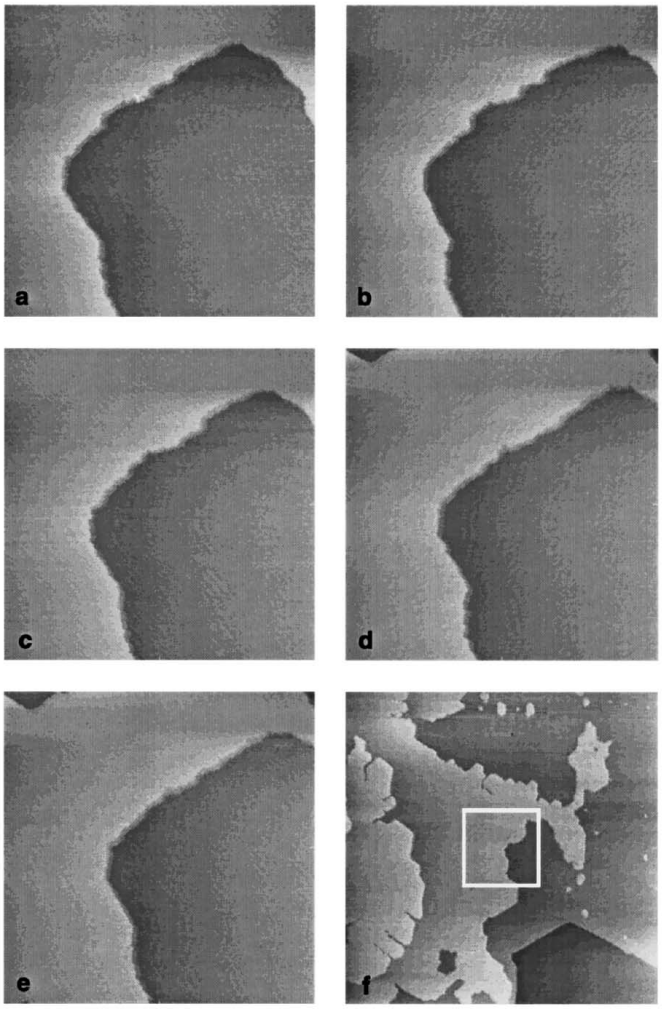

FIG. 5. (a)–(e) Time-sequence images of a 500 nm × 500 nm area on Au(111) obtained at $E_e = -720$ mV. The images are 1 min apart and were acquired with $V_b = -50$ mV and $i_t = 10$ nA. (f) A 2 μm × 2 μm scan obtained after recording (e).

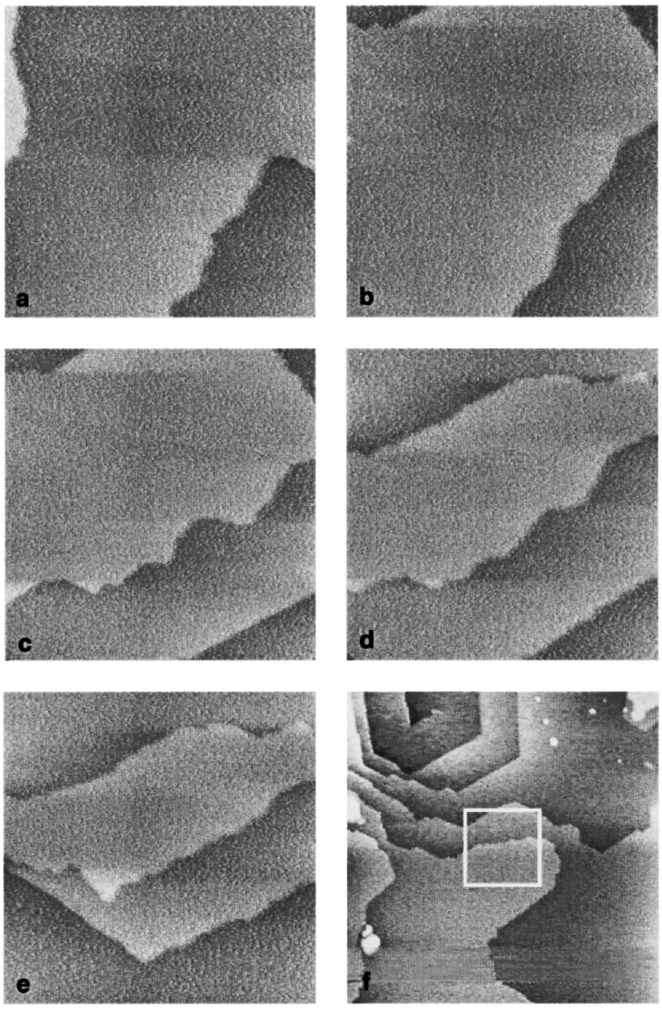

FIG. 6. (a)–(e) Time-sequence images of a 500 nm × 500 nm area on Au(111) obtained at $E_e = -720$ mV. The images are 1 min apart and were acquired with $V_b = 50$ mV and $i_t = 10$ nA. (f) A 2 μm × 2 μm scan obtained after recording (e).

D. Surface passivation by SAMs

To study the effect of surface passivation by an ultrathin, organic film, we modified the Au(111) surface in an ethanolic solution of $HS(CH_2)_{15}CH_3$ for 24 h. Previous results have demonstrated that this treatment results in a nearly defect-free film about 25 Å thick.[5–9,24,25] Figure 7(a) shows a 1 μm × 1 μm STM image of a SAM-coated Au(111) surface ($E_e = -770$ mV) in a 0.1 M KOH + 1 mM CN^- electrolyte solution obtained at −770 mV. Although they are not clearly resolved in this large-scale image, we observe the widely reported 2–5-nm-diam. pits randomly distributed within the monolayer.[10–12,15,17–19] The chemical and physical nature of these pits is still under debate, but we believe they are single-atom-deep defects in the Au lattice induced by the organomercaptan adsorption process.[38] The feature in the lower left-hand corner of the image is due to an intentional tip crash; we use it here as a positional marker.

After obtaining Figure 7(a), we moved the electrode potential from −770 to −520 mV, but we did not observe any significant change in the surface topography, even after the surface was scanned constantly for 5.5 min [Figure 7(b)]. This is in contrast to the behavior we noted on the naked Au(111) surfaces where fast etching occurred under similar conditions [Figs. 3(a) and 3(b)]. Even the step edges, which are among the most easily attacked surface features, remain undisturbed on the SAM-coated surface. In a duplicate companion experiment, we increased the CN^- concentration in the cell to about 15 mM but still did not observe any signs of Au etching at potentials as positive as −220 mV.

After acquiring Figure 7(b), we zoomed into a 100 nm × 100 nm portion of a Au terrace and scanned this area aggressively [Figure 7(c)]. The high tunneling current (10 nA) undoubtedly results in the tip being very close to the Au surface. Under these conditions rapid degradation of the monolayer occurs and the 2–5-nm-diam pits originally present within the SAM expand under the influence of the STM tip. After acquiring Figure 7(c), we scanned the same region three more times using the same conditions, and then we zoomed back out and obtained Figure 7(d). Clearly evident is a 25-Å-deep pit that was not originally present [Figure 7(b)]. The shape of the pit is not square because of thermal drift. Figure 7(e) shows the same region of the surface

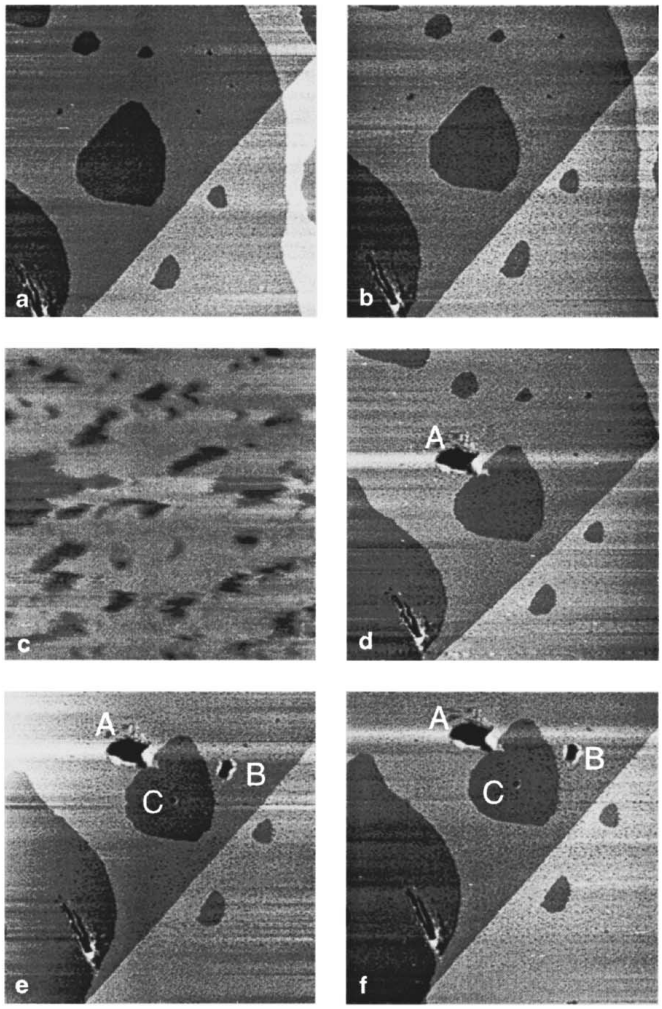

FIG. 7. Au(111) surfaces modified with $SH(CH_2)_{15}CH_3$ for 24 h and then imaged in a 0.1 M KOH + 1 mM KCN electrolyte solution. All images are 1 μm × 1 μm scans except that (c) is 100 nm × 100 nm. All the images were obtained with the tip potential fixed at −20 mV vs Ag/AgCl and i_t=200 pA except for (c): i_t=10 nA . E_e=−770 mV for (a)–(d) and E_e=−520 mV for (f). (a) Initial surface. (b) Image taken after the electrode potential was held at E_e=−520 mV for 5.5 min. (c) A 100 nm × 100 nm scan in a smaller area of (a). The tunneling current was set to 10 nA so as to open a square pit in the monolayer. (d) Image showing a hole that was generated by the high tunneling-current scans (4 scans). (e) Same region as in (d) after etching two additional pits nominally 50 and 10 nm square. (f) Same region as in (d) obtained after increasing the CN^- concentration to 5 mM and holding substrate potential at −520 mV for 4 min.

after etching two additional pits. Pits B and C are roughly 8 and 6 Å deep and nominally 50 nm and 10 nm square, respectively, suggesting that the lateral and vertical dimensions are connected. During the entire process of creating pits A, B, and C, the electrode potential was held at −770 mV where no CN^- etching of either a naked or SAM-coated Au surface occurs. After obtaining Figure 7(e), however, we increased the CN^- concentration to 5 mM and moved the electrode potential to −520 mV, conditions under which a naked Au surface rapidly dissolves, and then we scanned the surface 4 times using mild tunneling conditions. Figure 7(f) indicates no CN^- etching on either the unetched SAM surface or in the vicinity of the pits. That is, the depth of the previously STM-etched pits remained unchanged. Since CN^- must make intimate contact with Au prior to Au dissolution [Eqs. (1)–(3)], the bottoms of these pits must still be covered with corrosion inhibitors. We speculate that the Au in the bottom of these pits is coated with a monolayer of sulfur, which has been cleaved from the hydrocarbon tail of the organomercaptan, but at the present time we can only exclude the possibility of naked Au with certainty.

IV. CONCLUSIONS

We have studied F^-- and CN^--induced etching of naked Au(111) surfaces and Au(111) surfaces covered with passivating self-assembled monolayers of organomercaptans. Dissolution of the naked surfaces can be activated or deactivated by controlling the electrode potential. More interestingly, an as yet undefined tip-substrate interaction dramatically affects the dissolution rate. A positive tip bias accelerates dissolution of Au and a negative bias slows the etching. A full understanding of these phenomena awaits a better theoretical understanding of the properties of the electrolyte solution between the STM tip and the substrate.

We also found that Au surfaces modified with $HS(CH_2)_{15}CH_3$ for 24 h are completely passivated against CN^- etching even at high positive potentials. Importantly, disruption of the SAM by the STM tip does not lead to selective etching of the underlying surfaces. Even openings 25 Å deep are protected by an etch inhibiting agent, possibly an intact or partially fragmented organomercaptan. In contrast, results not discussed here explicitly indicate that Au surfaces modified with $SH(CH_2)_{15}CH_3$ for only 1 min, which are therefore only partially passivated, can be selectively etched by scanning while the rest of the surface is largely passivated. This indicates that poorly packed SAMs are less resilient corrosion barriers.

ACKNOWLEDGMENTS

The authors gratefully acknowledge the Office of Naval Research for full support of this work. We also thank Professor Allen J. Bard (University of Texas, Austin), Professor Reginald M. Penner (UC-Irvine), and Professor Henry S. White (University of Utah) for enlightening discussions.

[1]D. J. Trevor, C. E. D. Chidsey, and D. N. Loiacono, Phys. Rev. Lett. **62**, 929 (1989).
[2]R. L. McCarley and A. J. Bard, J. Phys. Chem. **96**, 7410 (1992).
[3]D. W. Suggs and A. J. Bard, J. Am. Chem. Soc. **116**, 10725 (1994).
[4]S. J. Chen, F. Sanz, D. F. Ogletree, V. M. Hallmark, T. M. Devine, and M. Salmeron, Surf. Sci. **292**, 289 (1993).
[5]R. G. Nuzzo and D. L. Allara, J. Am. Chem. Soc. **105**, 4481 (1983).
[6]R. G. Nuzzo, L. H. Dubois, and D. L. Allara, J. Am. Chem. Soc. **112**, 558 (1990).
[7]M. D. Porter, T. B. Bright, D. L. Allara, and C. E. D. Chidsey, J. Am. Chem. Soc. **109**, 3559 (1987).
[8]L. H. Dubois and R. G. Nuzzo, Annu. Rev. Phys. Chem. **43**, 437 (1992).
[9]C. D. Bain, E. B. Troughton, Y.-T. Tao, J. Evall, G. M. Whitesides, and R. G. Nuzzo, J. Am. Chem. Soc. **111**, 321 (1989).
[10]L. Sun and R. M. Crooks, J. Electrochem. Soc. **138**, L23 (1991).
[11]L. Sun and R. M. Crooks, Langmuir **9**, 1951 (1993).
[12]C. B. Ross, L. Sun, and R. M. Crooks, Langmuir **9**, 632 (1993).
[13]J. K. Schoer, C. B. Ross, R. M. Crooks, T. S. Corbitt, and M. J. Hampden-Smith, Langmuir **10**, 615 (1994).
[14]C. A. Widrig, C. Chung, and M. D. Porter, J. Electroanal. Chem. **310**, 335 (1991).
[15]Y. T. Kim and A. J. Bard, Langmuir **8**, 1096 (1992).

[16]Y.-T. Kim, R. L. McCarley, and A. J. Bard, J. Phys. Chem. **96**, 7416 (1992).
[17]C. Schönenberger, J. A. M. Sondag-Huethorst, J. Jorritsma, and L. G. J. Fokkink, Langmuir **10**, 611 (1994).
[18]J.-P. Bucher, L. Santesson, and K. Kern, Langmuir **10**, 979 (1994).
[19]T. Han and T. P. Beebe Jr., Langmuir **10**, 2705 (1994).
[20]G. E. Poirier and M. J. Tarlov, Langmuir **10**, 2853 (1994).
[21]S. J. Stranick, A. N. Parikh, Y.-T. Tao, D. L. Allara, and P. S. Weiss, J. Phys. Chem. **98**, 7636 (1994).
[22]R. M. Crooks, O. Chailapakul, C. B. Ross, L. Sun, and J. K. Schoer, in *Interfacial Design and Chemical Sensing*, edited by T. E. Mallouk, D. J. Harrison (American Chemical Society, Washington, DC, 1994), Vol. 561, p. 104.
[23]L. Sun, R. C. Thomas, R. M. Crooks, and A. M. Ricco, J. Am. Chem. Soc. **113**, 8550 (1991).
[24]S. E. Creager, L. A. Hockett, and G. K. Rowe, Langmuir **8**, 854 (1992).
[25]O. Chailapakul and R. M. Crooks, Langmuir **9**, 884 (1993).
[26]S. R. Snyder, J. Electrochem. Soc. **139**, 5 (1992).
[27]X. Gao, Y. Zhang, and M. J. Weaver, J. Phys. Chem. **96**, 4156 (1992).
[28]J. H. Schott and H. S. White, Langmuir **9**, 3471 (1993).
[29]C. Girard, C. Joachim, C. Chavy, and P. Sautet, Surf. Sci. **282**, 400 (1993).
[30]L. J. Whitman, J. A. Stroscio, R. A. Dragoset, and R. J. Celotta, Science **251**, 1206 (1991).
[31]U. Staufer, R. Wiesendanger, L. Eng, L. Rosenthaler, H. R. Hidber, H.-J. Güntherodt, and N. Garcia, J. Vac. Sci. Technol. A **6**, 537 (1988).
[32]J.-L. Huang, Y.-E. Sung, and C. M. Lieber, Appl. Phys. Lett. **61**, 1528 (1992).
[33]K. J. Cathro and D. F. A. Koch, J. Electrochem. Soc. **111**, 1416 (1964).
[34]D. W. Kirk, R. R. Foulkes, and W. F. Graydon, J. Electrochem. Soc. **127**, 1962 (1980).
[35]D. W. Kirk and F. R. Foulkes, J. Electrochem. Soc. **127**, 1993 (1980).
[36]D. M. MacArthur, J. Electrochem. Soc. **119**, 672 (1972).
[37]S. A. Hendricks, Y.-T. Kim, and A. J. Bard, J. Electrochem. Soc. **139**, 2818 (1992).
[38]O. Chailapakul, L. Sun, C. Xu, and R. M. Crooks, J. Am. Chem. Soc. **115**, 12459 (1993).